

Effect of Hole Doping on the London Penetration Depth of $\text{Bi}_{2.15}\text{Sr}_{1.85}\text{CaCu}_2\text{O}_{8+\delta}$ and $\text{Bi}_{2.1}\text{Sr}_{1.9}\text{Ca}_{0.85}\text{Y}_{0.15}\text{Cu}_2\text{O}_{8+\delta}$

W. Anukool^{1,2}, S. Barakat¹, C. Panagopoulos^{1,3,4} and J. R. Cooper¹

¹*Physics Department, University of Cambridge, Cambridge CB3 0HE, UK*

²*Physics Dept., Chiang Mai University, Thailand, 50200*

³*Department of Physics, University of Crete and FORTH, 71003 Heraklion, Greece,*

⁴*Department of Physics and Applied Physics, Nanyang Technological University, Singapore*

(Dated: Submitted 20th October 2008, Revised 10th June 2009)

We report measurements of AC susceptibility and hence the in-plane London penetration depth on the same samples of $\text{Bi}_{2.15}\text{Sr}_{1.85}\text{CaCu}_2\text{O}_{8+\delta}$ and $\text{Bi}_{2.1}\text{Sr}_{1.9}\text{Ca}_{0.85}\text{Y}_{0.15}\text{Cu}_2\text{O}_{8+\delta}$ for many values of the hole concentration (p). These support the scenario in which the pseudogap weakens the superconducting response only for $p \lesssim 0.19$.

I. INTRODUCTION

It is generally accepted that there is a pseudogap (PG) in the low energy excitation spectrum of hole-doped cuprate superconductors, with a definite energy scale ($E_G \equiv k_B T^*$) that falls as the hole concentration p is increased. However the details are controversial and a recent review¹ gives equal weight to three possible scenarios: (A) $T^*(p)$ falls to zero on the over-doped side together with the superconducting transition temperature $T_c(p)$, (B) $T^*(p)$ falls sharply to zero for slightly over-doped samples with $p \simeq 0.19$ or (C) $T^*(p)$ is similar to case (B) but there is no PG in the superconducting state. The p -dependences of the heat capacity⁴, and the in-and out-of-plane penetration depths, λ_{ab} and λ_c , of two grain-aligned single layer cuprates^{5,6} suggest that at low T the condensation energy⁴ and the superfluid density^{5,6} fall abruptly below $p \simeq 0.19$. This seems to support scenarios of type B, but the issue is still being debated^{1,2,3}. Here we report AC susceptibility (ACS) data⁷ showing how the in-plane superconducting penetration depth λ_{ab} of $\text{Bi}_{2.15}\text{Sr}_{1.85}\text{CaCu}_2\text{O}_{8+\delta}$ (Bi:2212) and $\text{Bi}_{2.1}\text{Sr}_{1.9}\text{Ca}_{0.85}\text{Y}_{0.15}\text{Cu}_2\text{O}_{8+\delta}$ (Bi(Y):2212) changes between $p = 0.08$ and 0.21 . These are relatively straightforward measurements, on the same unaligned sample as a function of δ , that can easily be checked by other research groups. We believe that they also support scenarios of type B above. They also give a linear T - dependence of $1/\lambda_{ab}(T)^2$, over a wide range of T , possibly becoming “super-linear” for pure Bi:2212 below 20 K. Combining our large values of $\lambda_{ab}(0)$ at low p with recent scanning tunnelling spectroscopy (STS) work⁸, suggesting relatively large Fermi arcs for $T_c = 20$ and 45 K, may also give important insights into cuprate superconductivity.

II. EXPERIMENTAL DETAILS

X-ray powder diffraction (XRD) patterns for the two samples in Fig. 1a. show that the Bi:2212 sample was phase pure to within the noise level of $2 - 3\%$. Two peaks that are not indexed arise from the incommensurate

TABLE I: Annealing conditions, hole concentrations and room temperature thermopower for Bi:2212 and Bi(Y):2212 samples. For both powder and bulk samples Eqn. 1 has been used to find p from T_c measured by ACS, with $T_c^{max} = 87.2 \pm 0.3$ K for Bi:2212 and 89.3 ± 0.3 K for Bi(Y):2212. The measured values of the room temperature thermoelectric power, $S(290)$ are also shown, and give consistent values of p .

Quench	Anneal conditions	p (holes/CuO ₂)		$S(290)$ ($\mu\text{V}/\text{K}$)
		Powder	Bulk	
Bi:2212				
Q1	300°C, 100%O ₂ , 7days	0.207	0.208	-6.32
Q2	400°C, 100%O ₂ , 24h	0.194	0.196	-4.18
Q3	450°C, 100%O ₂ , 23.5h	0.188	0.187	-3.06
Q4	500°C, 100%O ₂ , 24h	0.182	0.181	-1.81
Q5	600°C, 100%O ₂ , 23.5h	0.160	0.162	1.91
Q6	550°C, 80ppmO ₂ , 24h	0.154	0.160	3.24
Q7	620°C, 80ppmO ₂ , 24h	0.148	0.146	4.98
Q9	580°C, Vacuum, 24h	0.124	0.123	11.25
Q13	650°C, Vacuum, 22h	0.105	0.105	15.06
Bi(Y):2212				
Q1	300°C, 100%O ₂ , 7days	0.182	0.181	-2.2
Q3	350°C, 100%O ₂ , 24h	0.172	0.170	-0.63
Q4	425°C, 100%O ₂ , 24h	0.160	0.160	1.39
Q6	550°C, 100%O ₂ , 24h	0.151	0.148	5.90
Q8	550°C, 10%O ₂ , 30h	0.144	0.140	7.11
Q10	600°C, 80ppmO ₂ , 24h	0.121	0.120	14.24
Q11	540°C, Vacuum, 24h	0.098	0.099	25.25
Q12	600°C, Vacuum, 24h	0.088	0.094	28.73
Q15	650°C, Vacuum, 24h	0.082	0.087	33.64

superstructure⁹. They are also present for Bi(Y):2212 but this has two more peaks from 3-5% Bi₂O_{2.5} or Bi₂O₃. Examples of how the oxygen content of the sintered and powder samples was varied by annealing in flowing gases and quenching into liquid nitrogen¹⁰ are given in Table 1. Sample weights were measured immediately after quenching. p values were obtained from the T_c values measured by ACS using the parabolic law¹²:

$$\frac{T_c}{T_c^{max}} = 1 - 82.6(p - 0.16)^2 \quad (1)$$

Fig. 1b¹¹ shows p vs. cumulative weight changes for 11

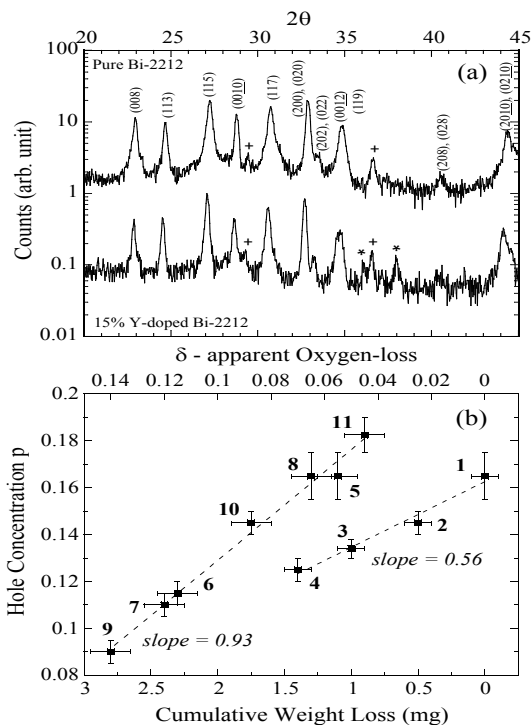


FIG. 1: (a) powder Cu $K\alpha$ XRD patterns for Bi:2212 and Bi(Y):2212 on a logarithmic scale. Impurity lines from $\text{Bi}_2\text{O}_{2.5}$ or Bi_2O_3 are marked by (*) and incommensurate satellite reflections⁹ by (+). (b) p is plotted vs. weight loss - lower scale and apparent oxygen loss - upper scale. Heat treatment details are given in footnote 13. p values were found from the ACS T_c of a sintered Bi(Y):2212 bar using Eq. 1 and $T_c^{max} = 89.1 \pm 0.3 K$.

annealing treatments on one of the sintered Bi(Y):2212 samples. After the initial irreversible changes (steps 1-4), the data are reversible and give a line of unit slope¹³. This provides further experimental confirmation¹² of the changes in p during the quenching treatments, because oxygen in the Sr-O Bi-O reservoir layer is expected to be O^{2-} and there are 2 Cu atoms per formula unit. Fig. 1b also shows that the irreversible losses ($\approx 1 \text{ mg}$ in 1.1 g) occurred continuously on heating from 450 to 550°C ¹³ and do not affect the value of p (since the p values at steps 1 and 5 are the same). Loss of Bi is the most likely cause since such a weight loss is equivalent to 0.004 Bi per formula unit and for a valency Bi^{4+} this would only change p by 0.008 - well within the error bars of points 1 and 5 in Fig. 1b.

Fine powders were obtained by gently grinding 50 - 100 mg of the fully-oxygenated sintered material with a small pestle and mortar. Two series of ACS experiments on Bi(Y):2212 powders gave similar results, data shown in Table 1 and Figs. 2b and 3b are for the second set. After the final (13th) quench, grain sizes were determined by measuring the dimensions of ~ 500 grains in a scanning electron microscope (SEM) photograph. Ap-

proximately $1/3$ of the grains were not circular and for these the geometric mean of the two radii was used. For Bi(Y):2212 the grain radius (r) at 50% cumulative volume (CV) was $1.5 \mu\text{m}$, with $r = 0.53$ and $2.20 \mu\text{m}$ at 10 and 90% CV respectively. For pure Bi:2212 the powders were sedimented in acetone to remove large particles, giving $r = 0.65$, 0.31 and $1.01 \mu\text{m}$ for the 50, 10 and 90% CV points respectively.

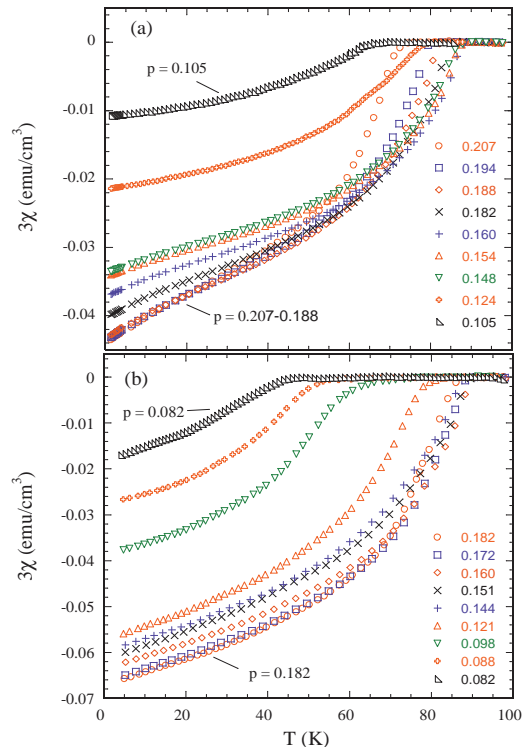


FIG. 2: Color on-line: volume susceptibility $\chi(T)$ vs. T for (a) pure Bi:2212 and (b) 15% Y-doped Bi:2212. The p values determined from T_c are also shown.

ACS measurements were made using standard techniques¹⁴. In the limit where λ_c is much larger than both λ_{ab} and the grain size, we can obtain λ_{ab} since only the component of H along the crystalline c - axis will give rise to detectable diamagnetism. In this case the AC signal from randomly oriented grains is $1/3$ of that for aligned grains with $H \parallel c$, because the average of $\cos^2 \theta$ over a sphere is $1/3$. Therefore we simply multiply the observed AC signal by 3 and apply our usual analysis for aligned grains^{6,15} with $H \parallel c$. The ACS data in Figs. 2a and 2b are in emu/cm^3 . Multiplying by $8\pi/3$ gives m/m_{max} where the magnetic moment m is reduced from m_{max} for a perfectly diamagnetic sphere because of the finite value of λ_{ab} . Allowing for a finite value of λ_c has negligible effect¹⁶.

The ACS signals in Fig. 2 were extrapolated linearly to zero to find T_c giving $T_c^{max} = 87.2 \pm 0.3 K$ for Bi:2212 and $89.3 \pm 0.3 K$ for Bi(Y):2212, and p values were then found using Eq. 1. We note that the lower values of

p in Table 1 were obtained by vacuum annealing which gives less control than using flowing gases. We believe that these samples are nevertheless uniformly doped for following reasons. (i) the samples were periodically re-oxygenated, e.g. between quenches Q9 and Q13 and Q12 and Q15 in Table 1, and the results showed that the vacuum anneals did not cause any irreversible changes. (ii) At 600°C oxygen diffusion in Bi:2212¹⁷ is so fast that the oxygen content in a $10\ \mu\text{m}$ diameter grain will attain uniformity in 1 second. (iii) The hole concentrations in Table 1 obtained from T_c for powders and sintered bars are very similar and agree with p values determined from the room temperature thermoelectric power using the results of Ref. 18. Such good agreement would not be obtained if the oxygen content of the powder samples were substantially non-uniform.

The raw ACS data in Fig. 2 clearly show that the signal, i. e. λ_{ab} , only changes strongly with p on the underdoped side for $p \leq 0.19$ and that for the Bi:2212 sample it saturates for $p \geq 0.188$. Also the well-defined onsets in the ACS signals at T_c are consistent with the finite size scaling analysis of specific heat data¹⁹, that ruled out gross inhomogeneity at any doping level. For Bi:2212 there is an increase in the slope of the diamagnetism below $20\ \text{K}$ for $0.15 < p < 0.21$, but this is not visible for the Y-doped samples over the range of p values studied, nor for lightly Zn-doped Bi:2212 samples ($T_c^{max} = 84\ \text{K}$ ⁷ - data not shown here).

III. ANALYSIS AND DISCUSSION

The data in Figs. 2a and 2b have been analyzed in the usual way by summing London's expression $m/m_{max} = 1 - 3\frac{\lambda}{a} \coth \frac{a}{\lambda} + 3\frac{\lambda^2}{a^2}$ for a superconducting sphere of radius a over the measured particle size distribution and varying λ until m/m_{max} equalled the measured value. The resulting values of λ_{ab} are plotted as $1/\lambda_{ab}^2$ vs. T in Figs. 3a and 3b. For Bi(Y):2212, $1/\lambda_{ab}^2$ vs. T is linear from low T up to T_c for $p = 0.12$ to 0.183 while for pure Bi:2212 there is evidence for "super-linear" behavior. Most of the data are slightly more linear than expected for a weak coupling BCS d -wave state, as shown in the insets to Fig. 3. A recent compilation based on various techniques¹ suggests that $2\Delta_{max}(0)$ is usually $\sim 5k_B T_c$ rather than the weak coupling value $4.28k_B T_c$ ²⁰. So we would not expect large deviations from weak coupling d -wave, but, if anything, larger gaps near the nodes would cause a slower decrease in $1/\lambda_{ab}^2$ with T at low T . The T -dependence for Hg:1223²¹ is close to that for weak coupling d -wave, but a slightly faster, more linear decrease was observed for YBa₂Cu₃O₇²² and more recently for heavily under-doped YBa₂Cu₃O_{6+x} crystals²³. Relatively few over-doped materials have been studied so the "super-linear" behavior could be a general property of clean over-doped cuprates. Note that $\lambda_{ab}(T)$ has only been reported for optimally-doped Bi:2212 crystals^{24,25} and in Fig. 3a the "super-linear" behavior is less marked in this case, i. e. for p

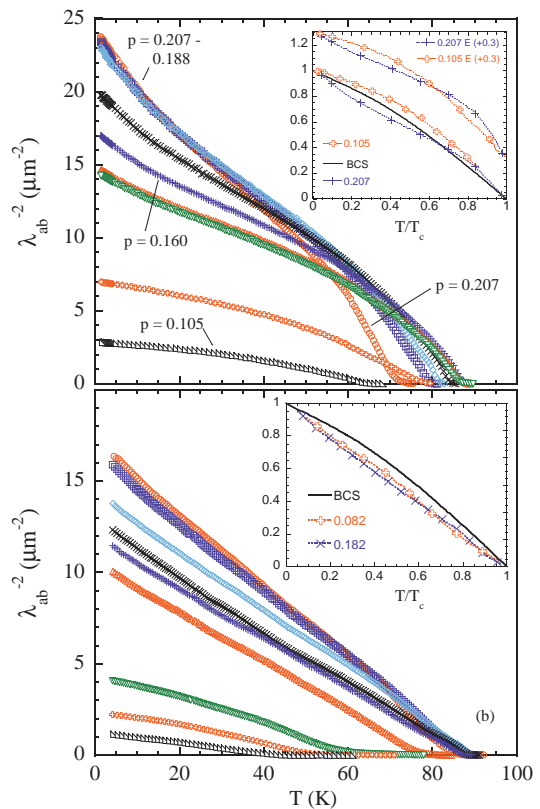


FIG. 3: Color online: the superfluid density ($n_s \propto 1/\lambda_{ab}^2$) plotted as a function of T for (a) pure Bi:2212 and (b) 15% Y-doped Bi:2212. Values of p are the same as in Fig. 2. Comparisons with weak coupling d -wave behavior for the highest and lowest values of p are shown in the insets. Results assuming 3:3:1 ellipsoids (E) with $H \parallel$ to the short side, instead of spheres, are also shown in the upper inset. Here $\lambda_{ab}(0)$ values are factors of 1.23 and 1.1 larger than for spheres for $p = 0.207$ and 0.105 respectively.

$= 0.16$. However SEM pictures⁷ of the sintered samples studied here showed that the crystallites of pure Bi:2212 were especially thin and plate-like, $\sim 0.3\ \mu\text{m}$ thick, while those of Bi(Y):2212 were much thicker. It possible that this is could be partly responsible for the "super-linear" behavior, as indicated in the inset to Fig. 3a, where results for an analysis based on ellipsoids with 3:3:1 aspect ratios are shown. So although the "super-linear" dependence is potentially an important result it needs to be confirmed by other measurements.

Generally speaking $1/\lambda^2$ is related to the low energy quasi-particle weight. If this were preferentially distributed near the nodes of the d -wave superconductor in k -space then $1/\lambda^2$ would indeed rise at low temperature as observed. Alternatively we note that the two chain cuprate, YBa₂Cu₄O₈ shows a similar "super-linear" behavior which was ascribed to superconductivity induced in the chains by the proximity effect at low T ²⁶. This raises the intriguing possibility that the pairing inter-

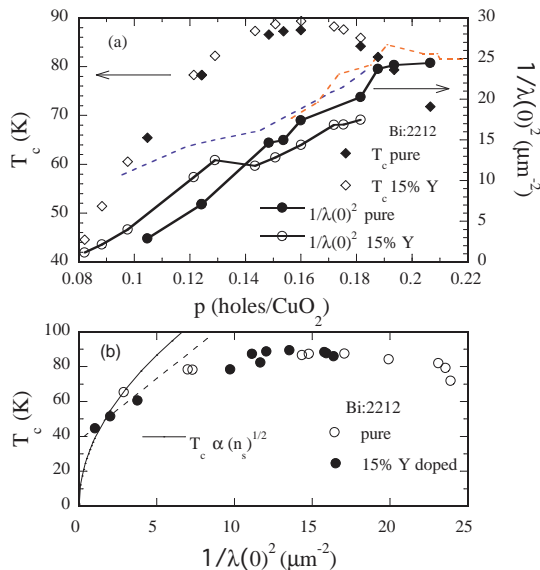


FIG. 4: Color on-line: (a) T_c and λ_0^{-2} are plotted vs. p . The red and blue dashed lines show data from heat capacity work²⁸. (b) Plot of T_c vs. $\lambda(0)^{-2}$, i.e. $n_s(T \rightarrow 0)$. The dashed line shows a linear variation while the solid line shows $T_c \propto \sqrt{n_s(0)}$ ²³.

action in Bi:2212 is very k -dependent and that for overdoped Bi:2212 samples, proximity coupling could be playing a role even for states within the Cu-O_2 planes.

In Fig. 4a data for both samples show a strong linear increase in $1/\lambda_{ab}^2(0)$ with p for $p \lesssim 0.19$ but $1/\lambda_{ab}^2(0)$ suddenly becomes constant for $p \gtrsim 0.19$. Bearing in mind that $1/\lambda_{ab}^2(0)$ is a measure of the superfluid density $n_s(0)$ as $T \rightarrow 0$ this strongly supports scenario B for $T^*(p)$. As shown in Fig. 4b there is a region where T_c increases linearly with $n_s(0)$, but the large intercept at $T_c = 40$ K means that the empirical Uemura relation, $T_c \propto n_s(0)$,²⁷ does not apply here. The solid line shows that at low p our data are more compatible with $T_c \propto \sqrt{n_s(0)}$ found recently for $\text{YBa}_2\text{Cu}_3\text{O}_{6+x}$ ²³ although for our Bi:2212 samples the values of $n_s(0)$ are much smaller for similar values of T_c . The plot in Fig. 4b is qualitatively consistent with the PG model of Ref. 28 but the initial increase of T_c with $n_s(0)$ in our data seems to be too sudden to give quantitative agreement. As also shown in Fig. 4a our direct measurements of $\lambda_{ab}(0)$ are consistent with earlier results²⁸ from a mean-field, Ginzburg-Landau (GL) analysis of the field-dependent heat capacity, except at low p where we find smaller values of $n_s(0)$. This is probably because of the large error bars in $n_s(0)$ obtained from the heat capacity at low p where the superconducting contribution is small²⁹. In Fig. 4a, the deviation of the two Bi(Y):2212 points at $p = 0.121$ and 0.129 from the general trend of $1/\lambda_{ab}^2(0)$ with p might be connected with a 1/8th plateau effect³⁰ in T_c . However simple modification of the $T_c(p)$ line near $p = 0.125$ will not account for

these two anomalous points.

Finally we briefly compare our results for $n_s(0)$ with recent STS data.⁸ $n_s(0)$ is a Fermi surface property and if the density of states $N(E)$ in the normal state is strongly energy (E) dependent it is expected²⁸ to be given by:

$$n_s(0) = \mu_0 e^2 \langle v_x^2 N(E) \rangle \quad (2)$$

where v_x is the projection of the Fermi velocity along the supercurrent direction and the average is taken over an energy range of the order of the superconducting gap. In a BCS-like d -wave situation this energy range will be $E_F \pm 3\Delta(\mathbf{k})$ where the product of the BCS parameters $u_{\mathbf{k}}$ and $v_{\mathbf{k}}$ is finite. The STS work suggests that for heavily underdoped Bi:2212 samples with T_c values of 20 and 45 K there are Fermi arcs (strictly speaking in the superconducting state these are Bogoliubov arcs) whose length in \mathbf{k} -space is still $\sim 1/3$ of that of the large hole-like Fermi surface seen in overdoped samples where there is no pseudogap. As the Mott insulating state is approached both techniques show a loss in density of states or spectral weight near E_F . But our results suggest that $n_s(0)$ is reduced by a factor of 25 when $T_c = 40$ K while at first sight the STS work only gives a factor of 3 reduction. Our data can be reconciled with STS if this loss of states also occurs in the region of the arcs, but over an energy range smaller than $E_F \pm 2 - 3\Delta(\mathbf{k})$, so that the Bogoliubov quasi-particle peaks are still visible in STS. This is qualitatively consistent with the model in Ref. 28 in which the PG is usually smaller than the superconducting gap. However we note that a microscopic theory of this effect also needs to consider what happens when a supercurrent is produced by uniformly displacing the Fermi surface in \mathbf{k} -space. Assuming that the PG is not displaced, then this continuity requirement seems to imply that only regions with a finite density of states at, and close to, E_F will contribute to the supercurrent.

IV. SUMMARY AND CONCLUSIONS

We report direct evidence that at low T the superfluid density of Bi:2212 falls rapidly for $p \lesssim 0.19$, which supports scenario B for the pseudogap in this widely-studied¹ compound. For both samples $1/\lambda_{ab}^2(0)$ is extremely small in the heavily under-doped region, down by a factor ≈ 25 while T_c remains relatively high ($T_c \simeq 40$ K). In conjunction with recent STS work⁸ this could be a useful constraint for theoretical models. For many values of p there is evidence for a linear T -dependence of the superfluid density over an unusually wide range of T and preliminary evidence for “super-linear” behavior below 20 K in over-doped samples of pure Bi:2212.

V. ACKNOWLEDGEMENTS

We acknowledge funding from the EPSRC (U.K.), for the experimental facilities in Cambridge, and further fi-

financial support from The Royal Society, EURYI, and MEXT-CT-2006-039047. W. A. was supported by the Development and Promotion of Science and Technology

Talents Project (D.P.S.T.), Thailand. We thank J. W. Loram, S. H. Naqib, J. L. Tallon and E. M. Tunnicliffe for helpful discussions.

-
- ¹ S. Hüfner, M. A. Hossain, A. Damascelli and G.A. Sawatzky, Rep. Prog. Phys. **71**, 062501 (2008).
- ² P. W. Anderson, Physica C **460-462**, 3 (2007).
- ³ Ø. Fischer, M. Kugler, I. Maggio-Aprile and C. Berthod, Rev. Mod. Phys. **79**, 353 (2007).
- ⁴ J. W. Loram, J. Luo, J. R. Cooper, W. Y. Liang and J. L. Tallon, J. Phys. Chem. Solids, **62**, 59 (2001).
- ⁵ C. Panagopoulos *et al.*, Phys. Rev. B **60**, 14617 (1999).
- ⁶ C. Panagopoulos, T. Xiang, W. Anukool, J. R. Cooper, Y. S. Wang and C. W. Chu, Phys. Rev. B **67**, 220502(R) (2003).
- ⁷ W. Anukool, PhD thesis, University of Cambridge, U.K. July 2003.
- ⁸ Y. Kohsaka *et al.*, Nature **454**, 1072 (2008).
- ⁹ A. Mironov *et al.*, JCPDS-International Center for Diffraction Data, 46-0431 (1998).
- ¹⁰ To prevent water vapor condensing on the samples after the quench, the gold sample container was placed in a glass beaker and warmed to room temperature by a strong stream of flowing gas. This procedure also worked well for the powder samples that were contained in a gold foil envelope but typically 1 - 2 mg were lost each time. All samples were periodically overdoped and re-measured to check that there had been no preferential loss of smaller or larger particles during the quench.
- ¹¹ S. Barakat, undergraduate summer project, University of Cambridge, (2000) unpublished.
- ¹² M. R. Presland, J. L. Tallon, R. G. Buckley, R. S. Liu, and N. E. Flower, Physica C **176**, 95 (1991).
- ¹³ The sequence is composed of 4 treatments in O₂ from 450 to 550°C, then 450°C in O₂ (5) and again at step 8. Treatments 6, 7, 9 and 10 correspond to various atmospheres, including vacuum, at temperatures up to 600°C, while 11 represents slow cooling from 450 to 100°C in O₂. After the initial heating to 550°C (steps 1-4) the data lie on the same reversible line. When referred to the oxygen content derived from the weight changes (top *x*-axis) this line has a slope of 0.93 ± 0.09.
- ¹⁴ A commercial (Lake Shore Model DRC-91CA) susceptometer and a homemade one with miniature coils of 2.6 mm internal diameter were used. The former was convenient for absolute magnitude and a wider range of AC fields while the latter could be used down to 1.3 K and gave smoother temperature dependences (absorption of paramagnetic oxygen can give spurious anomalies in magnetic susceptibility measurements between 40 and 60 K). They were calibrated by measuring pure lead (Pb) spheres at low enough frequencies (3.3 or 33.3 Hz) to have negligible eddy current signals in the normal state. The volume (*V*) of the powder was found from the weight and X-ray density (6.68 mg/mm³) and hence the signal (*m_{max}*) corresponding to an assembly of perfectly diamagnetic spheres could be found. In our experience the particles settle in the sample capsule so loosely that the magnetic interaction between grains is negligible, but in any case the demagnetization factor of the particles in their holder (the bottom of a gelatin capsule) is approximately 1/3, so the local field acting on any grain will be very close to the applied field¹⁵.
- ¹⁵ A. Porch, J. R. Cooper, D. N. Zheng, J. R. Waldram, A. M. Campbell and P. A. Freeman, Physica C **350-358** (1993).
- ¹⁶ The London equation $\nabla^2 B = B/\lambda^2$ is linear, so any diamagnetism arising from current loops that flow out of the *ab*-plane is additive. Since there are two in-plane axes, the appropriate averaging factor for out-of-plane currents and randomly oriented crystallites is 2/3. So for $\lambda_c \gg r$ there is an extra diamagnetic signal of $\frac{2}{3} \frac{3}{2} \frac{1}{4\pi} \frac{1}{15} r^2 / \lambda_c^2$ emu/cm³ in the measured susceptibility. With $r = 1 \mu\text{m}$ and $\lambda_c = 70 \mu\text{m}$ ³¹, this is only 3×10^{-6} emu/cm³ on the plots of Fig. 2. The effect would be negligible even if λ_c were a factor of 10 smaller. In our experience³² λ_c/λ_{ab} often follows the behavior of $\sqrt{\rho_c/\rho_{ab}}$ near room temperature, and this only decreases by a factor of 2 between $p = 0.16$ and $p = 0.20$ ³³.
- ¹⁷ T., M. Benseman, J. R. Cooper and G. Balakrishnan, Physica C **468**, 81 (2008).
- ¹⁸ S. D. Obertelli, J. R. Cooper and J. L. Tallon, Phys. Rev. B **46**, R14928 (1992).
- ¹⁹ J. W. Loram, J. L. Tallon and W. Y. Liang, Phys. Rev. B **69**, 060502(R) (2004).
- ²⁰ H. Won and K. Maki, Phys. Rev. B **49**, 1397 (1994).
- ²¹ C. Panagopoulos, J. R. Cooper, G. B. Peacock, I. Gameison, P. P. Edwards, W. Schmidbauer and J. W. Hodby, Phys. Rev. B **53**, R2999 (1996).
- ²² C. Panagopoulos, J. R. Cooper, N. Athanassopoulou and J. Chrosch, Phys. Rev. B **54**, R12721 (1996).
- ²³ D. M. Broun *et al.*, Phys. Rev. Lett. **99**, 237003 (2007).
- ²⁴ T. Jacobs, S. Sridhar, Q. Li, G. D. Gu and N. Koshizuka, Phys. Rev. Lett. **75**, 4516 (1995).
- ²⁵ S. F. Lee, D. C. Morgan, R. J. Ormeno, D. M. Broun, R. A. Doyle, J. R. Waldram and K. Kadowaki, Phys. Rev. Lett. **77**, 735 (1996).
- ²⁶ C. Panagopoulos, J. L. Tallon and T. Xiang, Phys. Rev. B **59**, R6635 (1999).
- ²⁷ Y. J. Uemura *et al.*, Phys. Rev. Lett. **62**, 2317 (1989).
- ²⁸ J. L. Tallon, J. W. Loram, J. R. Cooper, C. Panagopoulos and C. Bernhard, Phys. Rev. B **68**, 180501(R) (2003).
- ²⁹ J. W. Loram, Private communication, June 2009.
- ³⁰ Y. Koike, M. Akoshima, I. Watanabe and K. Nagamine, Physica C **341-348**, 1751 (2000).
- ³¹ J. R. Cooper, L. Forró and B. Keszei, Nature **343**, 444 (1990).
- ³² J. R. Cooper, H. Minami, V. W. Wittorff, D. Babič and J. W. Loram, Physica C **341-348**, 855-858 (2000).
- ³³ L. Forró, Phys. Lett. A **179**, 140-144 (1993).